JOURNAL OF SPACECRAFT AND ROCKETS
Vol. 43, No. 2, March–April 2006

# Mars Science Laboratory Parachute Simulation Model

Eric M. Queen* and Behzad Raiszadeh*
*NASA Langley Research Center, Hampton, Virginia 23681*

**A multibody flight simulation for the Mars Science Laboratory that includes six-degree-of-freedom rigid-body models for both the supersonically deployed and subsonically deployed parachutes has been developed. This provides a complete end-to-end simulation of the entire entry, descent, and landing sequence. The simulation provides attitude history predictions of all bodies throughout the flight as well as loads on each of the connecting lines. Other issues such as recontact with jettisoned elements (heat shield, backshell, parachute mortar covers, etc.), design of parachute and attachment points, and desirable line properties can also be addressed readily using this simulation. Time histories of the parachute line loads and the parachute and lander aerodynamic angles are presented. The simulation shows that the backshell does not recontact the lander after separation.**

## Introduction

A MULTIBODY flight simulation for the Mars Science Laboratory that includes high-fidelity models for both the supersonically and subsonically deployed parachutes has been developed. The Mars Science Laboratory will include an active hazard detection and avoidance (HDA) system designed to ensure a safe touchdown even in hazardous terrain, thus allowing safe landings in areas that would be considered too dangerous otherwise. Use of the HDA system places additional emphasis on accurate modeling of the parachute dynamics because the system depends critically on the exact orientation of the lander relative to the surface. The hazards to be avoided include rocks, craters, and large sloping terrain. The HDA system is currently envisioned to be composed of lidar and radar elements that map the local terrain and determine the location of safe landing zones. The information gathered from the sensors would be provided to the onboard guidance algorithm, which would modify the target point to avoid the detected hazards. To accurately model this HDA capability requires an accurate end-to-end simulation of the entire entry, descent, and landing (EDL) sequence. Flight simulation of spacecraft with parachutes is mathematically complicated and not easily characterized using point-mass or single rigid-body approaches. It involves multiple bodies, some of which are very flexible, flying in close proximity with significant interaction effects. Because the bodies fly so close to one another, the flowfield around each vehicle has an aerodynamic affect on the others. There are also direct, physical connections such as lines. These lines exert a tension force that is a function of both the relative positions and the relative velocities of the connected bodies. In previous Mars lander missions, a separate simulation was developed for the parachute portion of flight because the vehicle/parachute combination does not behave as a single rigid body during this part of the entry. This was the approach followed for Mars Pathfinder and Mars Polar Lander. The Mars Pathfinder and Mars Polar Lander parachute simulations were done in ADAMS.[1] ADAMS is a commercial-off-the-shelf program that is used to simulate the motions of multiple rigid bodies.

The goal of this work is to develop a multibody simulation of flight under a parachute incorporated into a larger simulation of the entire EDL sequence. In this work the parachute is treated as rigid body, with the interaction forces between the parachute and other rigid bodies included. A similar treatment was used to simulate Viking drop-test flights.[2] This approach was also applied to the Viking entry trajectory, but no other multibody end-to-end simulations have been performed for more recent Mars probes. By treating the parachute as a rigid body, it is possible to create an end-to-end simulation from the last trajectory correction maneuver before atmospheric entry to touchdown. This simulation will provide the attitude history predictions of all bodies throughout the flight, which is required to model the performance of the HDA subsystem. Other issues such as recontact with jettisoned elements (heat shield, backshield, parachute mortar covers, etc.), design of parachute and attachment points, and desirable line properties can also be addressed readily using this simulation.

Received 29 August 2002; revision received 1 August 2004; accepted for publication 1 February 2005. 

*Aerospace Engineer, Vehicle Analysis Branch, Aerospace Systems, Concepts, and Analysis Competency. Member AIAA.

## Entry, Descent, and Landing Sequence

The 2009 Mars Science Laboratory (MSL) mission described in this report performs a direct entry at Mars. The vehicle slows itself through atmospheric drag until about Mach 2.2, at which point a supersonic parachute similar to that used for Viking and Pathfinder is deployed. The geometry of the lander with a supersonic parachute deployed is shown in Fig. 1. When the vehicle is further slowed to Mach 0.8, the supersonic parachute acts as a drogue to deploy the subsonic parachute. The supersonic parachute and backshell are then jettisoned. After the subsonic parachute is fully deployed, the lander heat shield is jettisoned. The lander descends until its altitude is between 800 and 500 m. At an altitude determined by the onboard guidance, the lander separates from the subsonic parachute and descends to the surface under power of its main descent engines.

## Parachute Description and Modeling

The MSL EDL sequence addressed here uses two parachutes. The first, supersonic parachute is a disk-gap-band parachute based on the Viking, Pathfinder, and Mars Exploration Rover designs. It is 16.15 m in diameter. The second parachute is a more conventional, subsonic parachute with a diameter of 30.5 m. The aerodynamics of the parachutes are represented as coefficients of normal, axial, and side force. The normal- and side-force coefficients vary with angle of attack and are assumed to be equal because of the axial symmetry of the parachute. The normal-force coefficient of the parachute is shown in Fig. 2. The subsonic parachute was assumed to have the same normal- and side-force coefficients, but a different axial-force coefficient. The axial-force coefficient for the supersonic parachute is 0.61 while the axial-force coefficient for the subsonic parachute is 0.85 (Ref. 3). For each parachute, the inflation takes place over 1.3 s based on an inflation profile from Ref. 4. The inflation profile is shown in Fig. 3. This inflation ratio is used as a multiplier on each of the aerodynamic coefficients for each parachute, from the time of mortar fire until full inflation. The axial-force coefficients for both parachutes were assumed to be constant with Mach number. For both parachutes, it is assumed that the canopy and shroud lines form a single rigid body.

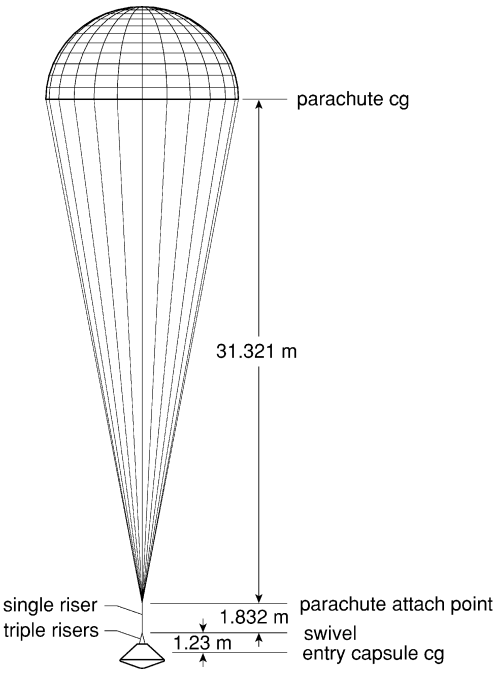


**Fig. 1 Mars Science Laboratory entry configuration.**

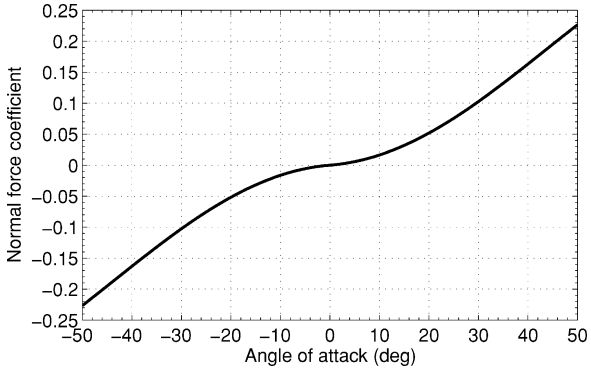


**Fig. 2 Normal-force coefficient vs angle of attack, MSL entry parachute phase.**

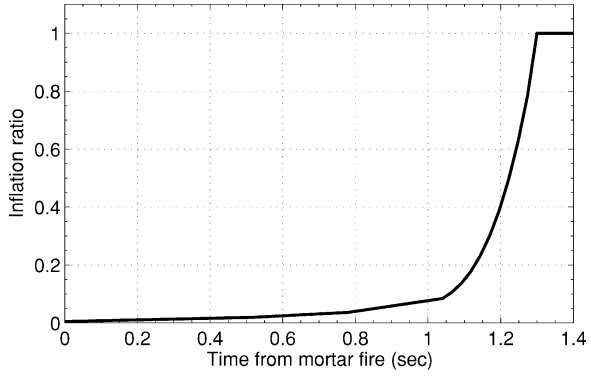


**Fig. 3 Parachute inflation vs time from mortar fire, MSL entry parachute phase.**

## Approach

The underlying simulation used for the Mars Science Laboratory is the Program to Optimize Simulated Trajectories II (POST II). POST II is the latest major upgrade to POST.[5] POST was originally developed for the space shuttle program to optimize ascent and reentry trajectories. Over the years it has been upgraded and improved to include many new capabilities. POST II relies on most of the technical elements established by POST, but the executive structure has been reworked to take advantage of today's faster computers. The new executive routines allow POST II to simulate multiple bodies simultaneously and to mix three-degree-of-freedom (DOF) bodies with six-DOFs-rigid bodies in a single simulation. The multibody capability allows POST II to simulate parachutes. The lines connecting the spacecraft and the parachutes are modeled as massless spring dampers. The springs can be attached at any point on the body. No moments are applied except those caused by force application away from the center of mass. Each line connects an attachment point on one body to an attachment point on another body and provides a tension-only force. When the lines are stretched, tension in the lines is determined as a function of strain and strain rate. Each of the spring-damper lines has an unstretched length, and if the separation distance between the two attach points is less than the unstretched length the line tension is zero.

For the results shown in this report, damping and stiffness were both assumed to be linear. For the single risers, both subsonic and supersonic, the stiffness used was 60,000 $\mathrm{N}\cdot\mathrm{m}$, whereas for the triple riser lines the stiffness was 47,000 $\mathrm{N}\cdot\mathrm{m}$. The damping in the single risers was 600 $\mathrm{N}\cdot\mathrm{m}\cdot\mathrm{s}$, whereas the damping in the triple risers was 470 $\mathrm{N}\cdot\mathrm{m}\cdot\mathrm{s}$. The unstretched length of the single riser was 1.832 m, whereas that of the triple risers was 0.71524 m. The triple risers were attached to a plate located 0.5356 m aft of the entry body c.g. Each riser was located 0.1714 m from the axis of symmetry of the vehicle, and the three triple risers were located symmetrically, each clocked 120 deg from the next.

To accurately target a selected site and to ensure that the parachute is deployed within its structural limits, onboard guidance and control systems are integrated into the simulation. The guidance system used is one based on a calculus of variations approach and is similar to the Apollo Earth-Return Terminal guidance. The guidance algorithm is described in detail in Ref. 6. The control system used is a phase-plane controller with each of the three axes controlled independently. The phase-plane controller is described in Ref. 7.

## Model Verification

To verify the multibody model as implemented in POST II, a series of increasingly complex tests were performed. These tests were intended to prove that the POST II model is implemented correctly by evaluating its performance on problems that could be verified by other means. The test cases started with a simple vertical drop from rest of the fully deployed parachute and entry body and gradually increased in complexity to include parachute opening, lander deployment, retrorocket firing, and other effects. The POST II model was compared to both MATLAB-based and ADAMS-based multi-DOFs simulations. In each case the agreement between the simulations was excellent. One of these test cases is excerpted next.

One of the test cases considered is a parachute deployment test. For this test case, the parachute has the same aerodynamics as the MSL supersonic parachute model used in this paper, but the diameter is only 15.07 m. The initial altitude is 8414.6 m with air-relative velocity of 500 m/s. The initial flight-path angle is $-30$ deg, and the initial azimuth is 90 deg. At the beginning of the simulation, the parachute is ejected by a mortar at 32 m/s relative to the capsule, giving the parachute an air-relative velocity of 468 m/s.

This case was implemented both into the POST II simulation and an ADAMS simulation. These two simulations are completely independent and use fundamentally different numerical approaches. The ADAMS simulation uses variable-step integration and does not allow any true discontinuities. Discontinuities are approximated using sigmoidal functions with steep slopes. POST II, on the other hand, has an event-based structure and uses a fixed-step integrator. This allows POST II to handle true discontinuities. Because of these fundamental differences, exact numerical agreement between POST II and ADAMS simulations would be extremely unlikely.

Figure 4 shows the line force for the single riser using both POST II and ADAMS. The line force is a good indicator of the agreement of the two simulations because it depends on both the relative position and relative velocity of the different bodies. If any of the bodies moves differently in one simulation than in the other, it will manifest itself as a different force, which will in turn cause the motion vary even more. The simulated line force profile is

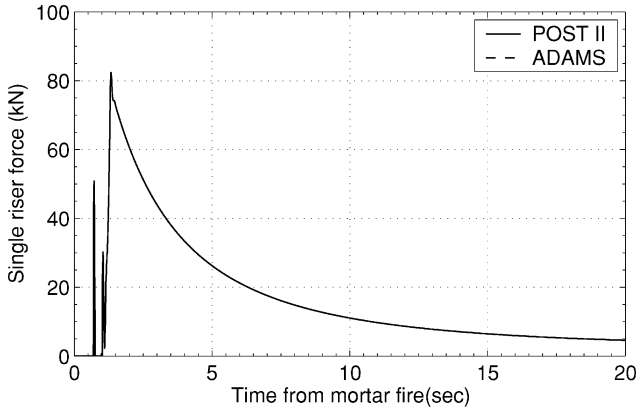


**Fig. 4 Single riser force using POST II and ADAMS.**

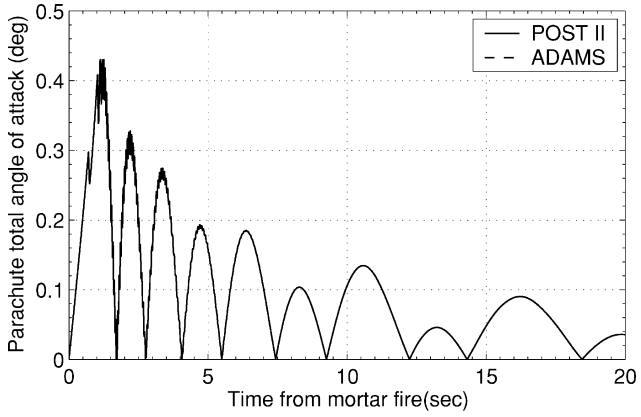


**Fig. 5 Parachute total angle of attack using POST II and ADAMS.**

essentially the same for both simulations; the final difference in force is less than 1 mN of a total force of 4600 N. Figure 5 shows the total angle of attack of the parachute from both simulations. The two curves are in very good agreement. The final difference in angle of attack between the two simulations is about $6.0 \times 10^{-5}$ deg.

Further examples of the agreement between the POST II and ADAMS simulations are beyond the scope of this report, but more of the verification and validation work is reported in Ref. 8. The complete set of test cases is due to be released in the near future as a NASA technical publication.

## Results

After completion of the verification phase, the specific parachute configuration of the Mars Science Laboratory has been incorporated into the simulation. This case begins 60 s prior to atmospheric entry. Atmospheric entry is assumed to occur at a radius of 3522.2 km. The initial velocity is 5.65 km/s, and the initial flight-path angle is −15.73 deg, leading to an entry flight path of −12.13 deg. When the vehicle is slowed to Mach 2.2 (approximately 480 m/s), the parachute is ejected from the back of the spacecraft by a mortar with a velocity relative to the spacecraft of 36.576 m/s. The parachute is held by a bag (assumed massless) until the lines connecting the parachute to the vehicle become taut, at which point the bag is discarded and the parachute begins to inflate. It is assumed that the inflation profile is a function of time only. Figure 6 shows the entry altitude as a function of velocity, and Fig. 7 shows a detail of the final part of the altitude velocity curve. As can be seen from Fig. 7, the backshell and supersonic parachute separate from the lander and subsonic parachute at Mach 0.8 (about 200 m/s). The backshell continues to the ground and impacts at about 40 m/s. The simulation ends when the lander reaches 500 m above ground level (3000 m above the reference ellipsoid), as that is the lowest altitude at which the guidance algorithm will command separation from the subsonic parachute. Figure 8 shows the line tension for four of the connecting lines as a function of time. The supersonic parachute

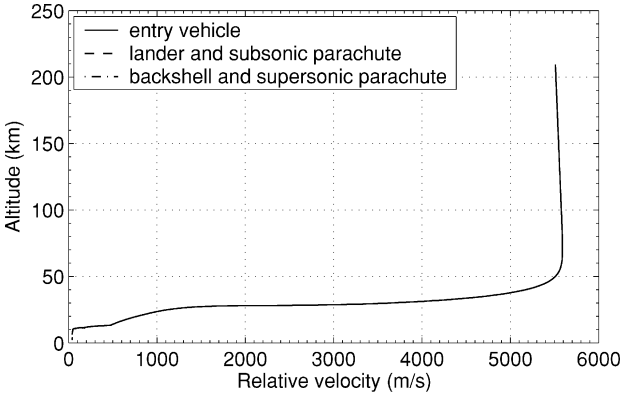


**Fig. 6 Entry altitude-velocity profile, MSL entry parachute phase.**

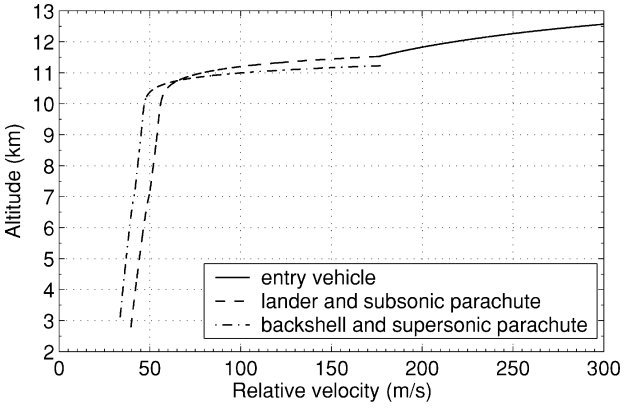


**Fig. 7 Detail of entry altitude-velocity profile, MSL entry parachute phase.**

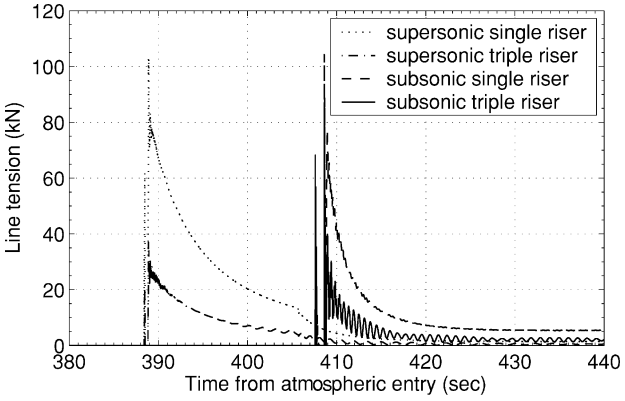


**Fig. 8 Parachute line tension around deployment, MSL entry parachute phase.**

deploys about 388 s after atmospheric entry, whereas the subsonic parachute deploys about 409 s after entry. In each case the triple riser loads are about 1/3 of the single riser loads.

Figure 9 is a detail from Fig. 8 showing the initial loads on the supersonic parachute single riser line. Also shown is the drag on the supersonic parachute. The force on the single riser is the summation of the parachute drag force and the inertial forces. In Fig. 9, the first peak (snatch load) is caused primarily by inertial forces, as the ejected parachute reaches the end of its line and rebounds, whereas the second, larger, peak is caused primarily by drag on the parachute during inflation (opening load). After the second peak, the drag force reduces as the vehicle slows and the dynamic pressure drops off.

The angle of attack of the entry vehicle and later the backshell is shown in Fig. 10. During the entry portion of flight before the parachute is deployed (about 390 s after entry), the angle of attack is constrained by the control system to remain near its trim angle of attack of about −15 deg. After the parachute is opened, the parachute

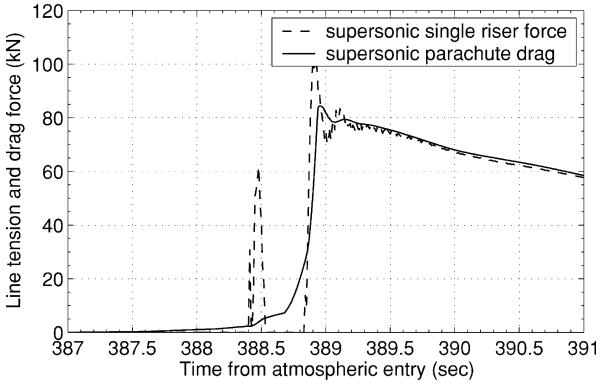


**Fig. 9 Line tension compared to drag force, MSL entry parachute phase.**

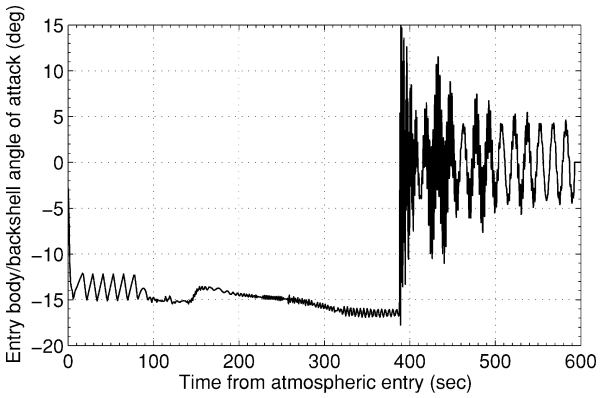


**Fig. 10 Entry body/backshell angle-of-attack history, MSL entry parachute phase.**

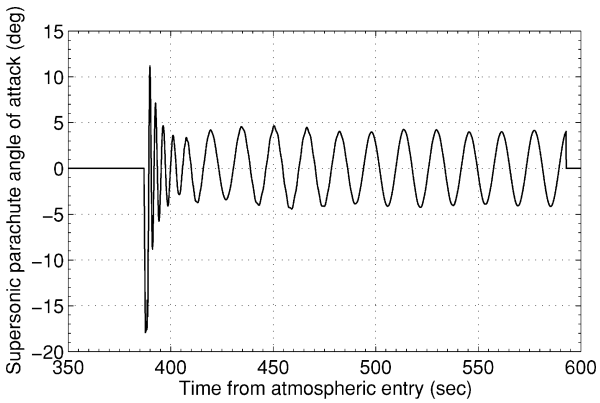


**Fig. 11 Subsonic parachute angle of attack, MSL entry parachute phase.**

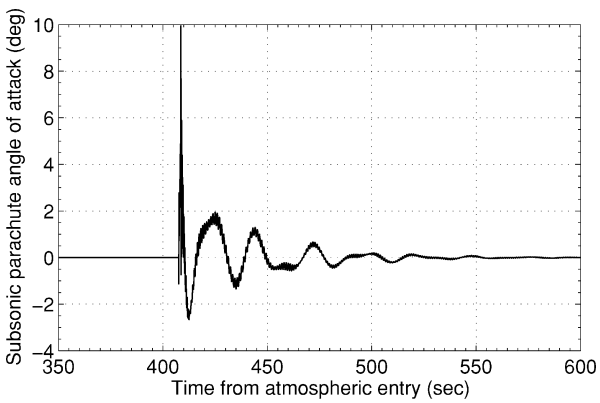


**Fig. 12 Supersonic parachute angle of attack, MSL entry parachute phase.**

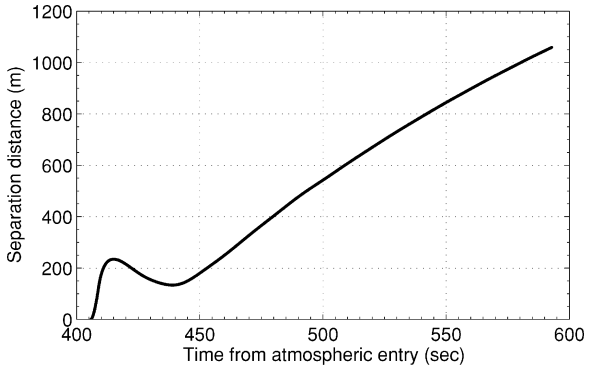


**Fig. 13 Separation distance between backshell and lander, MSL entry parachute phase.**

dominates the aerodynamics of the vehicle-parachute combination. The angle of attack of the entry body/backshell is determined by the dynamics of the parachute-lander system. Figures 11 and 12 show the angle of attack for the two parachutes. The supersonic parachute is seen to oscillate with an amplitude of about five deg while the subsonic parachute quickly settles to a constant angle of attack. The oscillation of the supersonic parachute might be because of the smaller load it carries. After about 409 s the supersonic parachute only supports the backshell.

The distance between the lander and the backshell is shown in Fig. 13. This figure shows that the two bodies separate, move toward each other, and separate again more permanently. In this case, recontact between the pieces was not an issue.

## Conclusions

A multiple rigid-body parachute simulation model for the Mars Science Laboratory entry phase has been developed. The model includes dynamics caused by interacting lines in a way that is easily incorporated into an end-to-end simulation of the entry phase. The model has been used to examine a nominal trajectory from entry until the lander drops from the subsonic parachute. The loads on each of the lines connecting the various bodies were calculated and found to be less than 120 kN for each line. It was seen that the line loads closely followed the parachute drag force, as expected. The main difference between the line load and the parachute drag was caused by inertial loads as the parachute was deployed. Finally, the separation distance between the lander and backshell was computed, and it was determined that, for this case, recontact was not an issue.

## References

[1]Smith, K. S., Peng, C. Y., and Behboud, A., "Multibody Dynamic Simulation of Mars Pathfinder Entry, Descent and Landing," Jet Propulsion Lab., D-13298, Pasadena, CA, April 1995.

[2]Talay, T. A., "Parachute-Deployment-Parameter Identification Based on an Analytical Simulation of Viking BLDT AV-4," NASA TN D-7678, Aug. 1974.

[3]Cruz, J. R., Mineck, R. E., Keller, D. F., and Bobskill, M. V., "Wind Tunnel Testing of Various Disk-Gap-Band Parachutes," AIAA Paper 2003-2129, May 2003.

[4]Ewing, E. G., Bixby, H. W., and Knacke, T. W., *Recovery Systems Design Guide*, Air Force Flight Dynamics Lab., AFFDL-TR-78-151, Gardena, CA, Dec. 1978.

[5]Powell, R. W., Striepe, S. A., Desai, P. N., Tartabini, P. V., Queen, E. M., Brauer, G. L., Cornick, D. E., Olson, D. W., Petersen, F. M., Stevenson, R., Engel, M. C., and Marsh, S. M., *Program to Optimize Simulated Trajectories: Volume II, Utilization Manual*, ver. 1.1.1.G, NASA Langley Research Center, Hampton, VA, May 2000.

[6]Carman, G., Ives, D., and Geller, D., "Apollo-Derived Mars Precision Lander Guidance," AIAA Paper 98-4570, Aug. 1998.

[7]Calhoun, P. C., and Queen, E. M., "Entry Vehicle Control System Design for the Mars Smart Lander," *Journal of Spacecraft and Rockets*, Vol. 43, No. 2, 2006, pp. 324–329; also AIAA Paper 2002-4504, Aug. 2002.

[8]Raiszadeh, B., and Queen, E., "Partial Validation of Multibody Parachute model in POST II," NASA TM-2002-211634, Oct. 2001.

M. K. Lockwood
*Guest Editor*